Nuclear Physics A373 (1982) 267–288

THE GROUND STATE OF DEFORMED NUCLEI AS A BOSON CONDENSATE

J. DUKELSKY, G.G. DUSSEL* and H.M. SOFÍA

Departamento de Física, Comisión Nacional de Energía Atómica, Av. del Libertador 8250, 1429 Buenos Aires, Argentina

Received 4 June 1981
(Revised 2 September 1981)

Abstract: It is shown that the ground state of deformed nuclei can be considered as a condensate of bosons that do not have a well-defined angular momentum. Values for the quadrupole moment and the particle number that are very close to the values obtained using the full boson wave function are obtained by retaining only the s- and d-parts of the boson wave function.

By comparing with the many-shell (realistic) situation we found the limitations of the single-shell calculations.

1. Introduction

The nuclear field theory [1]) (NFT) yields a description of a many-fermion system in terms of fermionic and bosonic elementary modes of excitation [2]), by treating perturbatively the coupling between both types of excitations. The convergence of the NFT near closed shells nuclei has been shown to be good in the Pb region [3]), but it is more and more difficult to apply the NFT as the number of particles (or excitations) outside closed shells increases.

The principal series approximation [4]) (PSA) is a method based on the NFT. It was initially developed for pairing-like interactions and it is based on the analytic properties of the matrix elements of any operator $\hat{\theta}$ as a function of the number of particles ($2M$) and the degeneracy of the shell† (Ω).

$$\langle f|\hat{\theta}|i\rangle = \sum_{nm} a_{nm}\left(\frac{M}{\Omega}\right)^n\left(\frac{1}{\Omega}\right)^m .$$

The series for the lowest value of m was called [4]) the principal series (PS) for the operator $\hat{\theta}$. In the PSA the one-body Green function PS (describing the fermionic excitations) is related self-consistently to the two-body Green function PS (asso-

* Fellow of the Consejo Nacional de Investigaciones Científicas y Técnicas, Buenos Aires, Argentina.

† The use of a single j-shell for the classification of the order of the diagrams in the PSA is equivalent to the use of two equally degenerate shells in the NFT [1]).

ciated with the bosonic degrees of freedom). The equations derived in this way are equivalent to the ones obtained in a self-consistent Hartree–Fock–Bogoliubov treatment.

The relation between these two PS is obtained by assuming that the ground state of the system is a boson condensate. This assumption is the central approximation made in the PSA. The condensate, and its coupling to the fermionic degrees of freedom (which are evaluated using the NFT type of rules), determine the structure of the fermionic excitations, which in turn define the microscopic structure of the bosons that condensate. (The angular momentum of these bosons may not be well defined.)

The physical image obtained in the PSA is different from the one usually obtained, for example with the BCS wave function in the description of superconductivity. In the PSA one knows which processes are included, and therefore it is formally possible to include higher-order corrections. For example, as in the PSA, the number of particles is conserved to the order of Ω to which the calculation is done; this number is conserved to leading order in Ω as in the BCS treatment, but by the inclusion of the proper diagrams it is possible to correct this non-conservation to the next order in Ω.

In the present paper we develop the PSA for a general interaction that also contains components of the multipole–multipole type. We discuss the application of the PSA to a single j-shell in detail because in this situation the equations simplify greatly and the physical content of the approximation does not change essentially as compared to the many-shell situation.

This schematic model (single j-shell) was used in ref. [5]) to analyze the interacting boson model and to compare the coupling scheme based on the alignment of individual particles in the deformed potential to the one based on the aligned bosons.

In sect. 2 we develop the PSA for a general force while in sect. 3 we apply it to one shell using some very simple schematic forces that display how the change between the coupling schemes discussed in ref. [5]) is obtained.

When evaluating the number of particles and the matrix elements for the quadrupole operator similar results are obtained by considering either the s- and d-components or the full wave function for the boson of the condensate. Therefore, even if the calculation is not done in the sd subspace only, the results obtained indicate that to consider only this subspace may be a quite good approximation.

The connection between this sd subspace and the one used in the interacting boson model [6]) (IBM) must be carefully done, because in the present treatment the inert core is formed by states that do not contribute to the Nilsson orbitals and it is smaller than the one used in the IBM (spherical closed shell), and it implies that the number of bosons to be considered when the system is deformed must be bigger than for the spherical case.

In sect. 4 we apply the PSA to the rare earth nuclei, allowing for a comparison of the results obtained in a single j-shell with the ones corresponding to a realistic set of single-particle energies, showing the limitations of the single j-shell calculation.

2. Procedure used

In this section we consider M pairs of fermions in one shell of degeneracy Ω interacting with a general two-body hamiltonian. It is useful to define two types of auxiliary operators:

$$P^+_{\lambda\mu} = \langle j \| Y_\lambda \| j \rangle [b^+_j b^+_j]^\lambda_\mu ,$$
$$Q_{\lambda\mu} = \langle j \| Y_\lambda \| j \rangle [b^+_j \bar{b}_j]^\lambda_\mu , \tag{2.1}$$

where b^+_{jm} creates a fermion in the state jm and $\bar{b}_{jm}$ transforms under rotations as (jm). In terms of these operators it is possible to write the most general hamiltonian in two alternative ways:

$$H_{\mathrm{PP}} = -\sum_\lambda \frac{\pi G_\lambda}{2\lambda+1} \sum_\mu P^+_{\lambda\mu} P_{\lambda\mu} ,$$
$$H_{\mathrm{PH}} = -\sum_\lambda \frac{\pi \chi_\lambda}{2\lambda+1} \sum_\mu Q^+_{\lambda\mu} Q_{\lambda\mu} . \tag{2.2}$$

In the PSA it is assumed that the ground state can be explained as a boson condensate. By that we mean M equal bosons interacting among themselves. For simplicity it will be assumed that the projection of the angular momentum onto the z-(intrinsic) axis is zero. In this picture, therefore, all deformed nuclei must be axially symmetric. It must be noted that in the Baranger and Kumar calculations [7]) almost all nuclei were axially symmetric (79 out of 82).

Therefore, the only effective part of the hamiltonian (2.2) in either forms is the one corresponding to $\mu = 0$, and are shown diagrammatically in fig. 1.

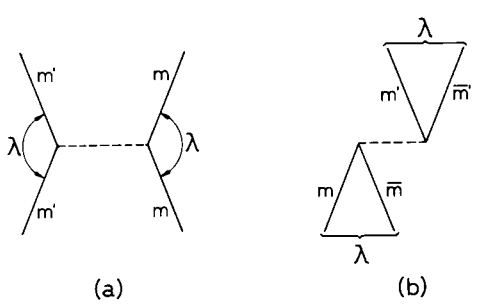

Fig. 1. Graphical representation of the hamiltonian matrix elements that must be included in a PSA calculation. (a) Particle–hole type, that corresponds to H_{PH}, (b) Particle–particle term, H_{PP} [see (2.2)].

The reason underlying the condensate assumption is that, when one of the external bosons is created or annihilated it contributes with a statistical factor $\sqrt{M}$ while, if the bosons are different, the M-dependence disappears.

In order to determine which diagrams belong to a PS it is necessary to isolate the factors introduced by the different parts of a diagram [4]). A boson can generate two

types of contributions: either $\sqrt{M/\Omega}$ if it belongs to the initial or final states (condensate), or $1/\sqrt{\Omega}$ if it is one of the internal bosons that appears only in the intermediate states. Each fermionic vertex yields a factor $1/\Omega$ while each loop carries a factor Ω.

It is seen therefore, that the principal series for a given process will be given by the set of diagrams where the number of connections (internal bosons or fermionic couplings) is as close as possible to the number of loops.

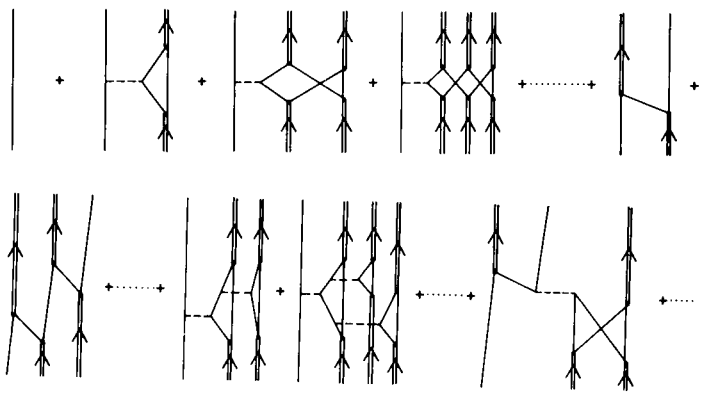

Fig. 2. Some of the PS diagrams that appear in the evaluation of the fermionic excitation energies.

Some of the diagrams corresponding to the principal series of the fermionic excitation energies are shown in fig. 2 while the ones corresponding to the creation of a bosonic excitation are shown in fig. 3.

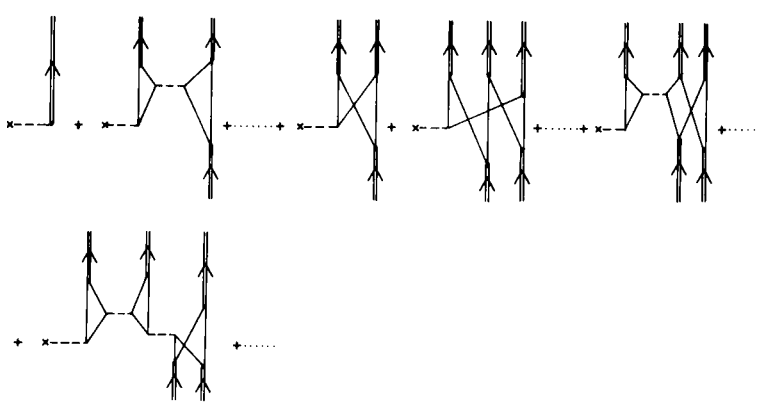

Fig. 3. Some of the PS diagrams that appear in the evaluation of the two-particle creation operators.

In order to sum up these diagrams it is convenient to define the fermionic excitation as in fig. 4. The partial summation done in fig. 4a allows us to express the elementary excitation as a Dyson-like equation (fig. 4b).

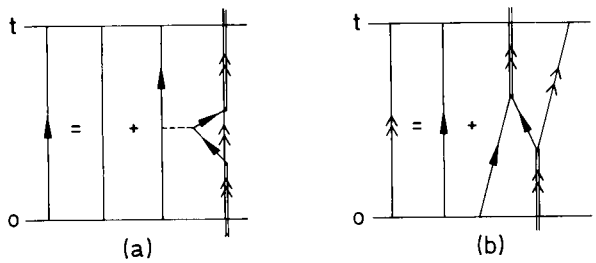

Fig. 4. PSA diagrams contributing to the one-body Green function. (a) Partial summation that is equivalent to the Nilsson hamiltonian. (b) Full Dyson equation for the excitations. In both cases the boson created or annihilated belongs to the condensate.

As in ref. [4]) the bosonic excitation is generated through the interaction of a particle (as defined in fig. 4a) and a quasiparticle† (as defined in fig. 4b). It follows upon inspection that the diagrams corresponding to the boson shown in fig. 5 are such that its creation corresponds to the diagrams shown in fig. 3.

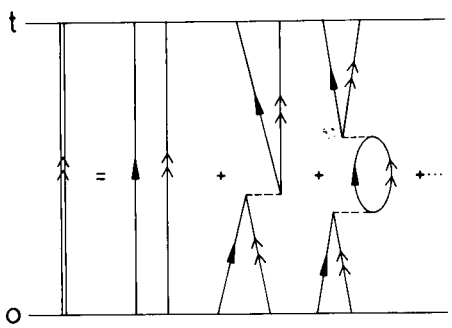

Fig. 5. Diagrams defining the microscopic structure of the boson in the PSA.

It must be noted that both forms of the hamiltonian (2.2) are relevant in different types of processes. H_{PH} only contributes to the description of the ground state through the diagram shown in fig. 4a. The topology of the diagrams when H_{PH} is considered is different from the one obtained by considering H_{PP} alone. It is therefore necessary to include simultaneously both hamiltonians without introducing any double counting to leading order in Ω. In the next order in Ω it should be necessary to make subtractions to many diagrams, for example the one shown in fig. 6.

The diagram in fig. 4a is equivalent to the HF approximation if the ground state is a boson condensate, and for this diagram it is more convenient to use the multipole particle–hole version of the hamiltonian. This allows the isolation of the effect of the

† Note that these quasiparticles are not equivalent to the ones defined through the Bogolyubov–Valatin transformation.

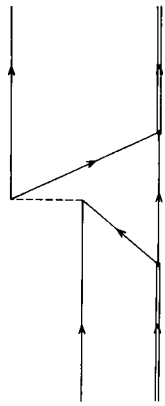

Fig. 6. Diagram of order $1/\Omega$ that was partially included in the order-1 diagram of fig. 4a.

$\hat{Q}_{\lambda\mu}$ operators on the vacuum and therefore diagram 4a corresponds to a Hartree–Fock insertion of the multipole–multipole interaction. The single-particle energies are

$$\varepsilon_m = -\sum_{\lambda} \pi\chi_\lambda \langle jm|\hat{Q}_{\lambda 0}|jm\rangle\langle\hat{Q}_{\lambda 0}\rangle\,, \tag{2.3}$$

where $\langle\hat{Q}_{\lambda 0}\rangle$ is the expectation value of $\hat{Q}_{\lambda 0}$ in the vacuum, as shown in fig. 7. Once the microscopic structure of the boson is known through the use of fig. 5, $\langle\hat{Q}_{\lambda 0}\rangle$ is evaluated through fig. 7. In a single j-shell the residues of the Green functions are equal to one, even if the equivalent of the Nilsson transformation has been done. The

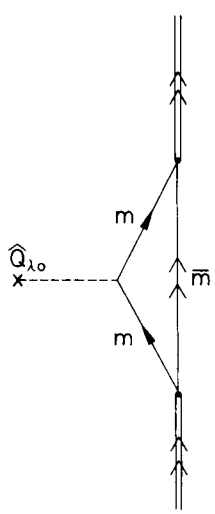

Fig. 7. Diagram corresponding to the diagonal matrix element of the quadrupole moment.

equation defining the fermionic excitations of the system (fig. 4b) must be worked out carefully because the boson propagator from $t=-\infty$ to $t=+\infty$ may cause some asymptotic problems. These problems can be avoided using the same techniques as in ref. [4]) or (with a trick that is based on the fact that the PSA is number conserving to each order in Ω) by changing the zero of the single-particle energies so that the two-body Green function shown in fig. 5 has a pole for zero energy. This implies that the boson propagator is

$$G_{\mathrm{B}}(t)=\theta(t)\,, \tag{2.4}$$

and that the equation associated with fig. 4b is

$$G_m(t)=G_m^{(0)}(t)-\Delta_m^2\int\!\!\int_{-\infty}^{\infty}\mathrm{d}t_1\,\mathrm{d}t_2\,G_m^{(0)}(t_2)G_{\bar{m}}^{(0)}(t_2-t_1)G_m(t-t_1)\,, \tag{2.5}$$

where the bosons appear only through their coupling constant Δ_m,

$$\Delta_m=\sqrt{M}\sum_{m'}\langle m\bar{m}|H|m'\bar{m}'\rangle\langle 0|b_{m'}b_{\bar{m}'}|n\rangle\,. \tag{2.6}$$

The factor $\sqrt{M}$ arises from the presence of M bosons and $\langle 0|b_{m'}b_{\bar{m}'}|n\rangle$ are the amplitudes for the two-particle states in the boson $|n\rangle$. Apart from the factor $\sqrt{M}$, (2.6) is the usual NFT recipe for the coupling constant between the fermions and bosons.

The spectral representation of the quasiparticle and particle Green functions,

$$\begin{aligned}G_m(t)=&\sum_a \mathrm{e}^{-iE_m^{(a)}t}\langle 0|b_m|a\rangle\langle a|b_m^+|0\rangle\theta(t)\\&-\sum_r \mathrm{e}^{-iE_m^{(r)}t}\langle 0|b_m^+|r\rangle\langle r|b_m|0\rangle\theta(-t)\,,\\ G_m^{(0)}(t)=&\,\mathrm{e}^{-i(\varepsilon_m-\lambda)t}\theta(t)\,,\end{aligned} \tag{2.7}$$

can be used to transform (2.5) into an algebraic equation. Performing its Fourier transform:

$$\begin{aligned}&\sum_a\frac{|\langle a|b_m^+|0\rangle|^2}{k-E_m^{(a)}}+\sum_r\frac{|\langle r|b_m|0\rangle|^2}{k-E_m^{(r)}}\\&\quad=\frac{1}{k-(\varepsilon_m-\lambda)}+\frac{\Delta_m^2}{k^2-(\varepsilon_m-\lambda)^2}\left\{\sum_a\frac{|\langle a|b_m^+|0\rangle|^2}{k-E_m^{(a)}}+\sum_r\frac{|\langle r|b_m|0\rangle|^2}{k-E_m^{(r)}}\right\}.\end{aligned} \tag{2.8}$$

As usual, the unknown residues and energies are obtained by studying (2.8) at its poles,

$$\frac{\Delta_m^2}{2(\varepsilon_m-\lambda)}\left[\sum_a\frac{|\langle a|b_m^+|0\rangle|^2}{(\varepsilon_m-\lambda)-E_m^{(a)}}+\sum_r\frac{|\langle r|b_m|0\rangle|^2}{(\varepsilon_m-\lambda)-E_m^{(r)}}\right]=-1\,, \tag{2.9a}$$

$$\sum_a \frac{|\langle a|b_m^+|0\rangle|^2}{\varepsilon_m - \lambda + E_m^{(a)}} + \sum_r \frac{|\langle r|b_m|0\rangle|^2}{\varepsilon_m - \lambda + E_m^{(r)}} = 0\,, \tag{2.9b}$$

$$[E_m^{(a)}]^2 = (\varepsilon_m - \lambda)^2 + \Delta_m^2\,. \tag{2.9c}$$

The addition poles $E_m^{(a)}$ corresponding to excitations in the system with $2M+1$ particles must be positive [8]) while $E_m^{(r)}$ must be negative. Therefore

$$E_m^{(a)} = -E_m^{(r)} = E_m = +\sqrt{(\varepsilon_m - \lambda)^2 + \Delta_m^2}\,, \tag{2.10}$$

while (2.9a) and (2.9b) give for the two states accessible from the ground state (one addition and one removal)

$$\begin{aligned} |\langle a|b_m^+|0\rangle|^2 &= \frac{1}{2}\frac{E_m + (\varepsilon_m - \lambda)}{E_m} = U_m^2\,, \\ |\langle r|b_m|0\rangle|^2 &= \frac{1}{2}\frac{E_m - (\varepsilon_m - \lambda)}{E_m} = V_m^2\,. \end{aligned} \tag{2.11}$$

The expectation value of the multipole operators (fig. 7) yields

$$\begin{aligned} \langle \hat{Q}_{\lambda 0}\rangle &= \sum_m \frac{\Delta_m^2 U_m^2}{(E_m + \varepsilon_m - \lambda)^2}\langle jm|\hat{Q}_{\lambda 0}|jm\rangle \\ &= \sum_m V_m^2 \langle jm|\hat{Q}_{\lambda 0}|jm\rangle\,. \end{aligned} \tag{2.12}$$

In the evaluation of this diagram one uses the fact that the fermion-boson coupling constant (fig. 8) is Δ_m, that each time a quasiparticle is created (or annihilated) one has to introduce its residues U_m and that the two energy denominators are equal to $(\varepsilon_m - \lambda + E_m)$ because the boson energy is zero. The passage to the second line is achieved using (2.11).

The set of equations (2.3), (2.10), (2.11) and (2.12) defines the fermionic excitations in terms of characteristics obtained from the boson, i.e. λ and Δ_m.

The propagator of the bosonic excitation shown in fig. 5 corresponds to the TDA of a particle and a quasiparticle. If

$$\nu_{mm'} = \langle m\bar{n}|H|m'\bar{m}'\rangle\,,$$

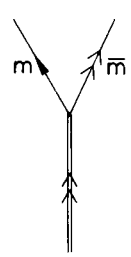

Fig. 8. Diagram corresponding to the amplitude of the particle–quasiparticle state in the PSA boson.

the Fourier transform of the TDA equation associated with fig. 5 can be written as

$$K_{mm'} = R_m \delta_{m,m'} + R_m \nu_{mm'} R_{m'} + \sum_{m''} R_m \nu_{mm''} R_{m''} \nu_{m''m'} R_{m'} + \cdots , \tag{2.13}$$

where R_m is the free propagator of a pair formed by a particle (m) and a quasiparticle ($\bar{m}$),

$$R_m(k) = \frac{|\langle a|b_m^+|0\rangle|^2}{k - (E_m + \varepsilon_m - \lambda)} . \tag{2.14}$$

Through the Lehman representation,

$$K_{mm'} = \sum_n \frac{\langle 0|b_m b_{\bar{m}}|n\rangle\langle n|b_{\bar{m}'}^+ b_{m'}^+|0\rangle}{k - E_n} , \tag{2.15}$$

the two-body Green function $K_{mm'}$ is expressed in terms of the residues ($\langle 0|b_m b_{\bar{m}}|n\rangle$) that appear in Δ_m [see (2.6)]. In order to obtain these residues we note that eq. (2.13) can be written in matrix form as

$$K_{mm'} = \left[\left(\frac{1}{R} - \nu\right)^{-1}\right]_{mm'} = [\mathbb{M}^{-1}]_{mm'} . \tag{2.13b}$$

If X_{rs} is the unitary matrix that diagonalizes $\mathbb{M}$ then we can rewrite (2.13b):

$$K_{mm'} = [X^{-1}]_{ms}\left[\frac{1}{X^{-1}\mathbb{M}X}\right]_{sr}[X]_{rm'} . \tag{2.13c}$$

If k is a pole of K, then the matrix $\mathbb{M}(k_n)$ has eigenvalue zero with eigenvector X_{mn}. If k is close to k_n then

$$\left[\frac{1}{X^{-1}\mathbb{M}X}\right]_{nn} = \frac{1}{(k - k_n)\left\{X_{nr}^{-1}\left[\left(\frac{\partial \mathbb{M}(k)}{\partial k}\right)_{k=k_n}\right]_{rs} X_{sn}\right\}} , \tag{2.16}$$

and by (2.15) and (2.13c) the residues are

$$\begin{aligned} \langle 0|b_m b_{\bar{m}}|n\rangle &= \frac{X_{mn}}{\left\{\sum_r X_{rn}\left[\frac{\partial 1/R}{\partial k}\right]_{rr'} X_{r'n}\right\}^{1/2}} \\ &= X_{mn}\left[\sum_r \frac{(X_{rn})^2}{|\langle a|b_r^+|0\rangle|^2}\right]^{-1/2} . \end{aligned} \tag{2.17}$$

It must be noted that the normalization of the residues is generated by (2.17) irrespective of the normalization of the X_{mn}.

λ must be chosen such that $k = 0$ is a pole of K, or in other words, such that the matrix $\mathbb{M}(k)$ has eigenvalue zero for $k = 0$. That yields the equation

$$\sum_{m'>0} \mathbb{M}_{mm'}(k=0) X_m = \frac{E_m + \varepsilon_m - \lambda}{|\langle a|b_m^+|0\rangle|^2} X_m + \sum_{m'>0} \nu_{mm'} X_{m'} = 0 . \tag{2.18}$$

Replacing the one-body residues given in (2.11) we obtain

$$X_m = -\frac{1}{2E_m} \sum_{m'>0} \nu_{mm'} X_{m'} . \tag{2.19}$$

The use of (2.17) and (2.6) shows that $X_m E_m$ is proportional to Δ_m with a constant that is independent of m. From (2.19) follows:

$$\Delta_m = -\sum_{m'>0} \nu_{mm'} \frac{\Delta_{m'}}{2E_{m'}} , \tag{2.20}$$

i.e. the usual gap equation obtained in the Hartree–Fock–Bogoliubov (HFB) theory. In terms of Δ_m the residues are

$$\langle 0|b_m b_{\bar{m}}|n\rangle = \frac{\Delta_m}{2E_m \{\sum_{m'>0} V_{m'}^2\}^{1/2}} . \tag{2.21}$$

The replacement of these residues in (2.6) together with the use of (2.20) yield the condition

$$M = \sum_{m'>0} V_{m'}^2 , \tag{2.22}$$

that is, the number equation.

Eqs. (2.3), (2.10), (2.11), (2.20) and (2.22) correspond to those obtained in the usual HFB treatment, but there is, nevertheless, a profound difference in the physical interpretation. As we have summed a principal series, i.e. all the processes corresponding to leading order in Ω for the different dynamical objects, the matrix elements of any operator are correct to leading order in Ω too. Moreover, it is possible to evaluate the next order in Ω at least for the lowest powers of M/Ω.

Another difference with the HFB treatment is the structure of the ground-state wave function [9]). The HFB wave function corresponding to the ground state has the form

$$|\tilde{0}\rangle_{\mathrm{HFB}} = D_0 \exp\left(\sum_{m>0} \frac{V_m}{U_m} b_m^+ b_{\bar{m}}^+ \right) |0\rangle , \tag{2.23}$$

where D_0 is a normalization constant and b_m^+ are the operators that create a particle in the states m, having an energy ε_m given by (2.3).

In our treatment the concept of wave function has not been used, but we have assumed that the ground state is a boson condensate, i.e.

$$|\tilde{0}\rangle_{\mathrm{PSA}} = D_0' (\Gamma_{\mathrm{PSA}}^+)^M |0\rangle . \tag{2.24}$$

The boson of the condensate is formed by a particle and a quasiparticle, and its wave function can be written as

$$\Gamma_{\mathrm{PSA}}^+ = \sum_{m>0} \lambda_m b_m^+ \beta_{\bar{m}}^+ , \tag{2.25}$$

where β_m^+ creates a quasiparticle [of the addition type, see eq. (2.7)]. The amplitudes λ_m can be obtained from fig. 8,

$$\lambda_m = \frac{\Delta_m U_m}{\sqrt{M}(E_m + \varepsilon_m - \lambda)} = \frac{V_m}{\sqrt{M}}. \tag{2.26}$$

The factor $1/\sqrt{M}$ appears because there is only one boson in fig. 8 while Δ_m is the coupling constant when there are M bosons present. The factor U_m is due to the quasiparticle residue.

The PSA boson may be expanded in terms of bosons that have a well-defined angular momentum

$$\Gamma^+_{\mathrm{PSA}} = \sum_J \left(\sum_{m>0} \frac{(-)^{j-m}}{\sqrt{M}} V_m \langle jjm - m | J0 \rangle \right) [b_j^+ \beta_j^+]_0^J$$

$$= \sum_J a_J [b_j^+ \beta_j^+]_0^J . \tag{2.27}$$

The expression for the coefficients a_J is different [10]) from that obtained by using (2.23). These coefficients can give information about the goodness of reducing the size of the space under consideration, i.e. by considering only the s- and d-parts of (2.27) as is done in the interacting boson model.

There are in particular two operators that are specially meaningful regarding this reduction of the space. One is the number of particles and the other is the quadrupole operator. The number of particles in the smaller space is given by

$$M_c = M(a_0^2 + a_2^2), \tag{2.28}$$

while in order to evaluate the quadrupole moment it is convenient to define

$$q_{JJ'} = \sum_m \langle jm | \hat{Q}_{20} | jm \rangle \langle jjm - m | J0 \rangle \langle jjm - m | J'0 \rangle .$$

The total quadrupole moment is given by

$$\langle \hat{Q}_{20} \rangle = M \sum_{JJ'} q_{JJ'} a_J a_{J'}, \tag{2.29}$$

and therefore if one only considers the sd space,

$$\langle \hat{Q}^c_{20} \rangle = M(2q_{02} a_0 a_2 + q_{22} a_2^2) \tag{2.29b}$$

is obtained.

Another operator relevant to the system under discussion is the two-particle transfer operator with angular momentum two and projection zero, i.e.

$$\hat{\mathbb{T}}^+_2 = [b_j^+ b_j^+]_0^2 . \tag{2.30}$$

Its matrix element between the ground-state bands will be given by

$$T_2 = \langle M+1|\hat{\mathbb{T}}^+_2|M\rangle = \sqrt{M}\sum_{m>0}\langle n|b^+_m b^+_{\bar{m}}|0\rangle\langle jjm-m|20\rangle = \sum_{m>0}\langle jjm-m|20\rangle\frac{\Delta_m}{E_m}. \tag{2.31}$$

The mean values $\langle Q_{20}\rangle$ and T_2 are very sensitive to the quadrupole part of the force and their relative magnitudes depend upon the fact that this quadrupole force is of the particle–hole or particle–particle type.

The comparisons of M with M_c and $\langle\hat{Q}^c_{20}\rangle$ with $\langle\hat{Q}_{20}\rangle$ yield information concerning the physical basis for the interacting boson model.

3. Single *j*-shell

The purpose of this section is to provide a qualitative understanding of the ground-state structure and its relation with the description given by the IBM.

The boson wave function (2.25),

$$\Gamma^+_{\mathrm{PSA}} = \sum_{m>0}\frac{V_m}{\sqrt{M}}b^+_m\beta^+_{\bar{m}}, \tag{3.1}$$

is not only correct in the spherical superconductive case, when $V_m = \sqrt{M/\Omega}$, or in the particle aligned state, when

$$V_m = \begin{cases} 1 & \text{if } m \geq \Omega - M \\ 0 & \text{otherwise}, \end{cases}$$

but can also be used in the intermediate cases. The aim of the present section is to show that the actual ground state corresponds to one of these intermediate structures.

It is always possible to make an angular momentum decomposition of the boson using eq. (2.27).

For the particle aligned state (Hartree–Fock solution for a pure quadrupole-quadrupole hamiltonian) one obtains

$$a^2_L = \left(\sum_{m=j}^{j-M+1}(-)^{j-m}\frac{\langle jjm-m|L0\rangle}{\sqrt{M}}\right)^2[1+(-1)^L]. \tag{3.2}$$

Fig. 9 shows the values of these probabilities for $L \leq 6$, when $\Omega = 8$ and $\Omega = 16$. Differences in the probabilities for the two values of Ω used display the importance of the $1/\Omega$ corrections.

At the beginning or the end of the shell the pairing interaction dominates, and then the boson is pure s, different from the aligned state boson. In the rest of the shell the probability of finding the boson with angular momentum zero or two is quite close to one, even in the absence of any pairing interaction. It follows that between 85% and 100% of the boson corresponds to the s- plus d-components.

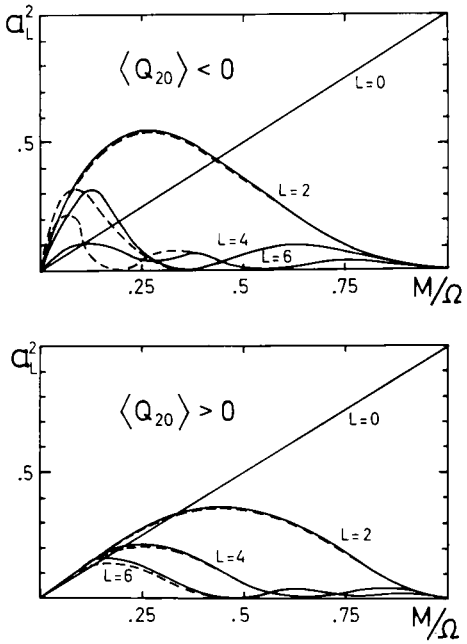

Fig. 9. Probability that the PSA boson has angular momentum L for the particle-aligned state with $L \leq 6$. The full line corresponds to $\Omega = 8$ and the dashed one to $\Omega = 16$. The probabilities were calculated for integral values of M and the lines are drawn to guide the eye.

In ref. [5]) a procedure to study a self-consistent description of the ground state considering only s- and d-bosons was developed.

Instead of doing this self-consistent type of approach we studied the behaviour of the system when only the s- and d-components of the boson wave function (3.1) are retained. In this case, it is useful to introduce the inverse relation to (3.2),

$$V_m = \sum_L a_L \sqrt{M} \langle jjm - m | L0 \rangle (-)^{j-m} . \tag{3.3}$$

Considering only $L = 0$ and $L = 2$ in the above equation, the space is cut into the s- and d-components of the boson, and in this way, a "cut-off probability" V_m^c is defined. Using V_m^c to evaluate matrix elements the only bosons involved in the processes are the s and d ones. Therefore, it is possible to evaluate N^c and $\langle \hat{Q}_{20}^c \rangle$ as:

$$N^c = \sum_m (V_m^c)^2 = 2M(a_0^2 + a_2^2) = N_0 + N_2 , \tag{3.4}$$

$$\langle \hat{Q}_{20}^c \rangle = \sum_m q_m (V_m^c)^2 = 2M \sum_{L,L'=0}^{2} a_L a_{L'} \sum_m q_m \langle jjm - m | L0 \rangle \langle jjm - m | L'0 \rangle . \tag{3.5}$$

Some qualitative understanding can be obtained solving the pairing-plus-quadrupole hamiltonian in a single shell with degeneracy $\Omega = 8$ and three pairs of

particles ($M = 3$). In order to determine the ratio between G_0 and X [$=\chi_2$ of (2.2)] that corresponds to the region of physical interest, it is possible to use that the residual interaction in nuclei has many similarities to a delta one, and therefore G_0 and X are essentially equal, as they are for the δ-force.

However, in a many-shells situation, the angular momentum selection rules make the quadrupole force more effective than in a one shell model, because it connects more states than the pairing interaction. So, it is reasonable to use for the ratio X/G_0 a number larger than one.

In ref. [5]) it was pointed out that another helpful parameter to determine the region of physical interest is $\delta\varepsilon/\Delta$ where $\delta\varepsilon$ corresponds to the spread in energy of the active single-particle states while Δ is the superconductive gap.

Table 1 shows the results obtained for some relevant quantities when the value of X/G_0 changes. We denote by T_J the matrix elements for the two-particle creation operator with angular momentum J, while $Q_{\max}$ is the quadrupole moment of the particle aligned system.

The agreement between the results obtained in the full space and those corresponding to the reduced space is good. The physically meaningful region can be considered as corresponding to $\delta\varepsilon/\Delta$ values between 3 and 10. In this region more than 95% of the boson wave function has zero or two units of angular momentum and the quadrupole moment is reasonably well-reproduced by the cut-off value.

In fig. 10 we show the values for V_m and V_m^c for different values of the ratio X/G_0. In the physical region the differences between them are small. As the value of X/G_0 increases, they change towards their (different) values in the particle aligned state. The pairing interaction is responsible for the similitude of V_m^c and V_m in the physical region.

4. The rare earth nuclei

In this section we apply the formalism of sect. 2 to the rare earth nuclei.

The first problem one is faced with is the election of the one- and two-body hamiltonians. In order to minimize the number of free parameters we choose the

TABLE 1

Results obtained in a shell with $\Omega = 8$ for $M = 3$ as X/G_0 is changed

$\frac{X}{G_0}$	$\delta\varepsilon/\Delta$	N_c/N	P_0	P_2	$\frac{\langle Q_{20}^c\rangle}{\langle Q_{20}\rangle}$	$\frac{\langle Q_{20}\rangle}{\langle Q_{\max}\rangle}$	$\frac{T_0}{\Omega}$	$\frac{T_2}{\Omega}$	$\frac{T_4}{\Omega}$
1.00	0	1.00	1.00	0			0.484	0	0
1.15	2.36	0.998	0.870	0.128	1.018	0.638	0.392	0.022	−0.061
1.45	6.23	0.980	0.694	0.286	1.051	0.883	0.259	0.012	−0.100
1.75	14.1	0.944	0.553	0.391	1.054	0.966	0.151	0.009	−0.082
2.05	2410	0.868	0.376	0.492	1.011	1.00	0.001	0.001	−0.001
∞	∞	0.868	0.375	0.493	1.010	1.00	0	0	0

$Q_{\max}$ is the value of $\langle\hat{Q}_{20}\rangle$ for the aligned particle state.

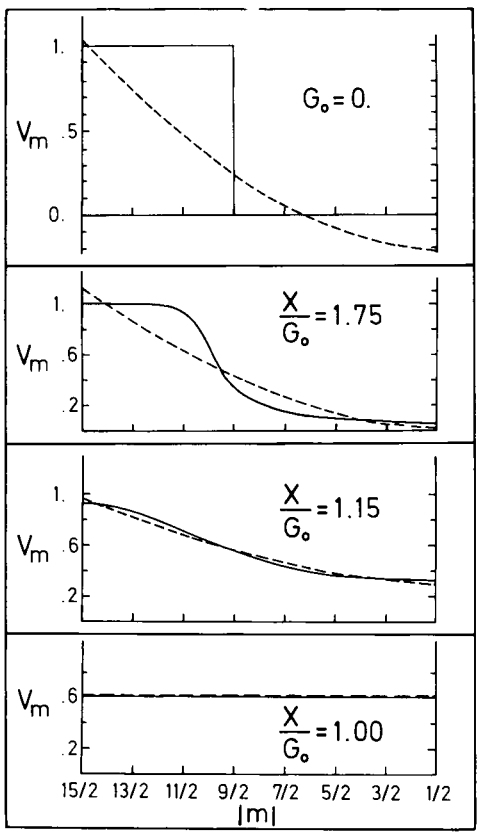

Fig. 10. Occupation numbers for different ratios of the quadrupole–quadrupole to the pairing forces. The full line corresponds to V_m and the dashed one to V_m^c. The calculation was done for $\Omega = 8$ and $M = 3$.

hamiltonian used by Kumar and Baranger [7]) in their self-consistent calculation of static shapes in the rare earth region. They gave the spectra of the one-body hamiltonian and a residual two-body term formed by the pairing (with angular momentum zero) plus quadrupole interactions with a definite strength for all the rare earth nuclei.

The second problem is the extension of the formalism developed in sect. 2 to a many-level situation. In this case the single-particle wave functions are different from the spherical ones but they can be related using the eigenfunctions of the Nilsson hamiltonian, i.e.

$$b^+_{\alpha m} = \sum_j R^{\alpha}_{jm} C^+_{jm}, \tag{4.1}$$

where C^+_{jm} creates a particle in an eigenstate of the one-body (spherical) hamiltonian while R^{α}_{jm} are the Nilsson amplitudes that are obtained doing the Hartree approximation for the single-particle plus quadrupole hamiltonian.

As the pairing interaction acts only between fermionic pairs having the same α-value, the structure of the PSA elementary boson will be similar to the one given in (2.25), i.e.

$$\Gamma^{+}_{\mathrm{PSA}} = \sum_{\alpha m} \lambda_{\alpha m} b^{+}_{\alpha m} \beta^{+}_{\alpha -m}\,, \tag{4.2}$$

where $\beta^{+}_{\alpha m}$ creates a quasiparticle (of the addition type). As in (2.25) $\lambda_{\alpha m}$ can be obtained using fig. 8 and therefore

$$\lambda_{\alpha m} = \mathrm{sig}\,(m)\frac{V_{\alpha|m|}}{\sqrt{2M}}\,. \tag{4.3}$$

The factor sig (m) accounts for the extra crossing present when $m<0$ as compared to the $m>0$ case.

The probability that the boson has a given angular momentum is obtained by expressing (4.2) in terms of the spherical states, i.e.

$$\begin{aligned}\Gamma^{+}_{\mathrm{PSA}} &= \sum_{\substack{j_1 j_2 \\ \alpha m}} \lambda_{\alpha m} R^{\alpha}_{j_1 m} R^{\alpha}_{j_2 -m} C^{+}_{j_1 m} \gamma^{+}_{j_2 -m} \\ &= \sum_{j_1 j_2 J} a_{j_1 j_2, J} [C^{+}_{j_1} \gamma^{+}_{j_2}]^{J}_{0}\,,\end{aligned} \tag{4.4}$$

where γ^{+} is associated with a spherical quasiparticle. The states (α, m) and $(\alpha, -m)$ will have the same energy because the hamiltonian used is invariant under time reversal. This implies a relation between both wave functions that can be expressed as

$$R^{\alpha}_{j-m} = (-)^{j-m} R^{\alpha}_{jm}\,. \tag{4.5}$$

This symmetry allows a simplified version of the coefficients in (4.4). Making use of (4.3) and (4.5) one obtains

$$a_{j_1 j_2, J} = \sum_{\alpha, m>0} \frac{V_{\alpha|m|}}{\sqrt{2M}} R^{\alpha}_{j_1 m} R^{\alpha}_{j_2 m} \langle j_1 j_2 m - m | J 0 \rangle (-)^{j_2 - m} [1 + (-)^{J}]\,. \tag{4.6}$$

This expression displays the fact that the boson only has non-zero probabilities for even angular momenta.

It must be noted that in ref. [9]) eq. (14) does not correspond to (4.6) and therefore the results that were reported there are not exact, even if the physical conclusions obtained there are corroborated when (4.6) is used.

The probability that the boson has angular momentum J is given by

$$P_J = \sum_{j_1 j_2} (a_{j_1 j_2, J})^2\,. \tag{4.7}$$

Figs. 11A and 11B show the P_0 and P_2 values, respectively, for the rare earth nuclei, while 11C displays the sum of all the other probabilities. The results shown

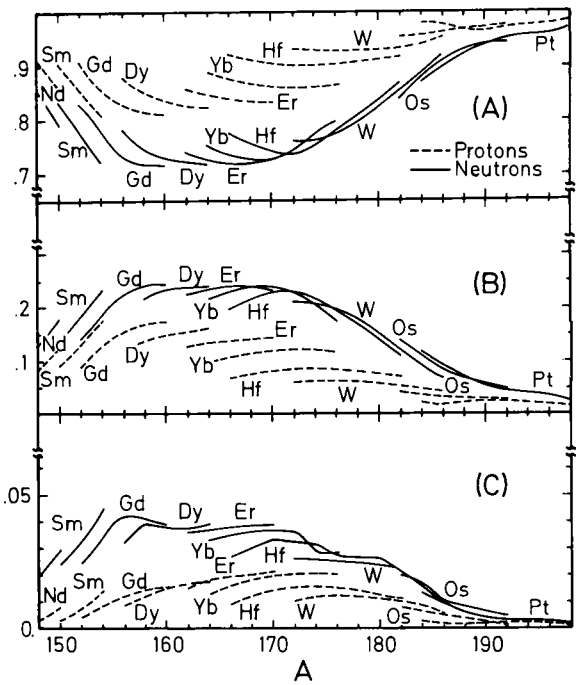

Fig. 11. Probabilities that in the rare earth nuclei the PSA boson has a given angular momentum. Probabilities are shown for (A) $J = 0$, (B) $J = 2$ and (C) $J \neq 0, 2$. In the ordinate is shown the mass number and each of the lines corresponds to a different element. The neutron values are linked by a full line while the dashed line corresponds to protons.

are slightly different from those reported in ref. [9]) because when P_2 is properly evaluated it turns out to be bigger than in ref. [9]) while P_0 retains the values reported there.

In table 2 are shown the P_J values corresponding to ^{154}Sm (which has the smallest $P_0 + P_2$) and to ^{170}Hf which can be considered a typical deformed nuclei.

If the BCS projected wave function is used instead of the PSA one, it is necessary to make the angular momentum decomposition of the boson replacing (4.3) by

$$\lambda_{\alpha m} = \mathrm{sig}\,(m)\frac{V_{\alpha|m|}}{U_{\alpha|m|}}C_0\,, \tag{4.3b}$$

where C_0 is a normalization constant. In fig. 12 are shown P_0, P_2 and the sum of all the other probabilities for the BCS projected wave functions. The results obtained in both treatments differ in the relative importance of P_0 and P_2, but in both cases their sums are almost the same and quite close to unity.

It is useful to reexpress (4.4) in its deformed version to evaluate the diagonal matrix elements of one body operators considering only the s- and d-amplitudes of

TABLE 2

The probability of different angular momenta inside the PSA boson for ^{154}Sm and ^{170}Hf

L	^{154}Sm		^{170}Hf	
	protons	neutrons	protons	neutrons
0	0.811	0.721	0.906	0.742
2	0.175	0.234	0.080	0.225
4	0.010	0.033	0.013	0.017
6	0.003	0.009	0.001	0.012
8	0.001	0.002		0.003
10		0.001		
12				

the boson, i.e.

$$\Gamma^{+}_{\mathrm{PSA}} = \sum_{\substack{j_1 j_2 m \\ J\alpha\alpha'}} a_{j_1 j_2, J} R^{\alpha}_{j_1 m} R^{\alpha'}_{j_2 - m} \langle j_1 j_2 m - m | J 0 \rangle ,$$

$$b^{+}_{\alpha m} \beta^{+}_{\alpha' - m} = \sum_{\alpha\alpha' m} W^{J_{\max}}_{\alpha\alpha', m} b^{+}_{\alpha m} \beta^{+}_{\alpha' - m} , \tag{4.8}$$

where

$$W^{J_{\max}}_{\alpha'\alpha m} = \sum_{\substack{J=0 \\ J=\text{even}}}^{J_{\max}} \left(\sum_{j_1 j_2} a_{j_1 j_2, J} R^{\alpha}_{j_1 m} R^{\alpha'}_{j_2 - m} \langle j_1 j_2 m - m | J 0 \rangle \right) . \tag{4.9}$$

When $J_{\max}$ is unrestricted, as we have made a unitary transformation and its inverse we obtain

$$W^{J_{\max}}_{\alpha\alpha', m} = \lambda_{\alpha, m} \delta_{\alpha, \alpha'} .$$

On the other hand, by making $J_{\max} = 2$ in (4.9) one considers only the s- and d-boson amplitudes.

By defining

$$(V^{c}_{\alpha, m})^2 = \sum_{\alpha'} (W^{J_{\max}=2}_{\alpha\alpha', m})^2 , \tag{4.10}$$

it is possible to write down the diagonal matrix element of any one-body operator making use of the diagram of fig. 7, (4.4) and (4.9),

$$\langle T^{c} \rangle = \sum_{\alpha m} (V^{c}_{\alpha, m})^2 \langle \alpha m | T | \alpha m \rangle . \tag{4.11}$$

Using this expression for the number of particles it yields

$$N^{c} = 2M(P_0 + P_2) ,$$

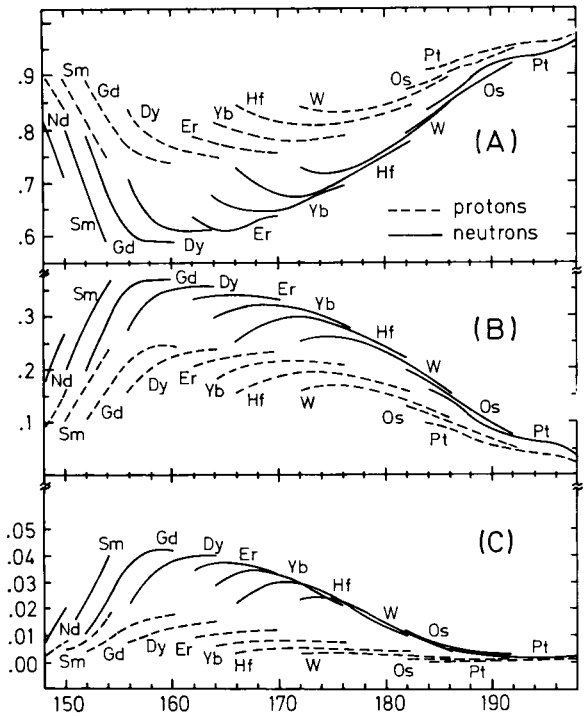

Fig. 12. Probabilities that in the rare earth nuclei the BCS boson has a given angular momentum. The conventions are as in fig. 11.

while the static quadrupole moment must be evaluated numerically. In fig. 13 is plotted the ratio between the value of $\hat{Q}_{20}$ obtained in this way as compared with its value obtained in the full space. The agreement between both results gives further support to the goodness of the procedure of considering only the s- and d-parts of the boson.

It is interesting to compare the coefficients $V^{c}_{\alpha m}$ with its uncut version $V_{\alpha m}$. This comparison results difficult because this last calculation is not self-consistent and in general $\langle \hat{Q}^{c}_{20} \rangle$ is different from $\langle \hat{Q}_{20} \rangle$. In this case one may wonder which are the single-particle energies (s.p.e) that must be used in a plot of $V^{c}_{\alpha m}$ as a function of the s.p.e. In fig. 14 we show the $(V^{c}_{\alpha m})$ as a function of the original Nilsson energies for two nuclei that partly illustrate this effect: in ^{150}Sm the quadrupole moment associated with the cut-off space is closer to the value obtained in the full space than in any other of the nuclei considered, while ^{184}Os can be thought of as having a typical departure between $\langle \hat{Q}^{c}_{20} \rangle$ and $\langle \hat{Q}_{20} \rangle$.

For ^{150}Sm the curve is smooth and shows a nice accord between the cut-off and full version of $V_{\alpha m}$, showing a small increase in the width of the region where $V_{\alpha m}$ goes from zero to one; while for ^{184}Os the ripples may be due to the difference between both $\langle \hat{Q}_{20} \rangle$.

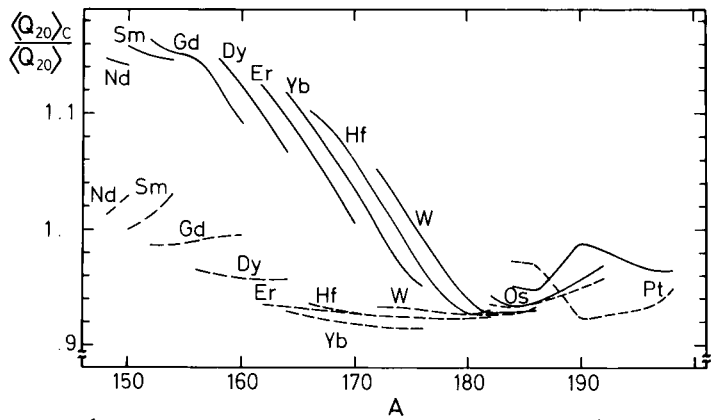

Fig. 13. Ratio of the $\hat{Q}_{20}$ matrix elements evaluated in the reduced space ($\langle\hat{Q}^c_{20}\rangle$) and in the full space ($\langle\hat{Q}_{20}\rangle$).

It is worthwhile to note that in the present treatment the coefficients $V^c_{\alpha m}$ can be larger than one, making unclear its physical meaning.

5. Conclusions

In this paper we have extended the PSA to deformed systems. The main physical assumption of this treatment is that the intrinsic ground state of a many-fermion

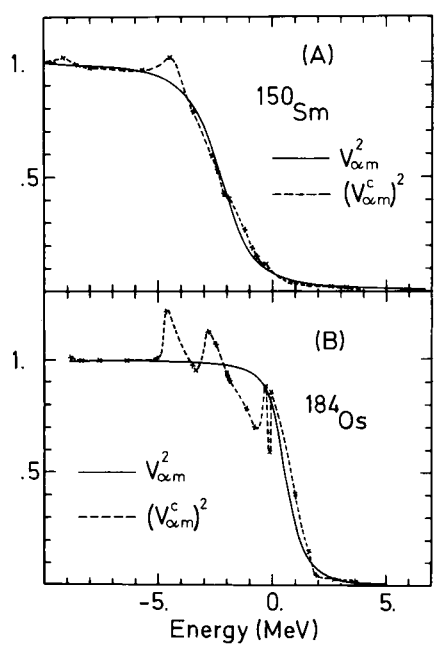

Fig. 14. Occupation probabilities for (A) ^{150}Sm and (B) ^{184}Os. The full line corresponds to $V_{\alpha m}$, the dashed to $V^c_{\alpha m}$.

system can be considered as a boson condensate. The procedure provides not only the boson wave function (that has a non-well-defined angular momentum) but relates it to the single-fermion excitation energies and "wave functions". There is no restriction upon the structure of the one- and two-body hamiltonians, and the main difference with the HFB description is the structure of the boson and of the ground state [see (2.23) and (2.24)]. In the PSA the matrix elements are evaluated using a state with a well-defined number of bosons, as is done in fig. 7 for one-body operators. On the other hand, in HFB the matrix elements are evaluated using its full wave function but if one only considers its projected part (having the right number of particles) the results are not reliable.

Once the PSA boson wave function is evaluated for the rare earth nuclei we consider the results that are obtained taking into account only the s- and d-amplitudes in the boson for two quantities: the number of particles and the static quadrupole moment. The comparison with the corresponding quantities obtained using the full boson wave function (see figs. 11 and 13) shows a good agreement between both evaluations. This agreement is only a necessary condition to assure that it is possible a description of deformed states by considering only s- and d-bosons (IBM). The only way to obtain a sufficient condition for the IBM is through a self-consistent calculation performed only with s- and d-bosons.

The results obtained in the single j-shell and its comparison with the many-shell situation clarify the limitations of this simple calculation. The first point is that the value of $\delta\varepsilon/\Delta$ to be used in the single j-shell depends upon the feature to be reproduced as compared with the realistic case. For example, the density of single-particle levels indicates that $3 \leqslant \delta\varepsilon/\Delta \leqslant 10$; the relation between $V^{c}_{\alpha m}$ and $V_{\alpha m}$ observed in the ^{150}Sm calculation (fig. 14) corresponds to values of $\delta\varepsilon/\Delta$ near 3; the amount of s-amplitude corresponds to $\delta\varepsilon/\Delta \simeq 6$ and the amount of non s- plus d-bosons corresponds to $\delta\varepsilon/\Delta \sim 10$.

It is well known [5]) that a self-consistent calculation in the single j-shell considering only s- and d-bosons yields different results for some physically meaningful quantities than does a similar calculation made in the full space. However the limitations that we found in the single j-shell calculation, as compared with the many-shell case, cast some doubts that the situation should necessarily be the same in a self-consistent calculation for a many- (non-degenerate) shell case.

In the present treatment the amount of s-amplitude is much higher than in other treatments, as noted by Otsuka [11]). This may be due to the fact that we have considered as inert core the states that do not appear in the construction of the Nilsson states. That means, for example, that our neutron core [7]) has only $N = 70$. Another reason, may be more fundamental, is that the amount of s-bosons depends critically on the strength of the pairing interaction as compared to the quadrupole one, and also on the degeneracy (or not) of the single-particle energies. The dependence on X/G_0 is shown in table 1 and the dependence on the single-particle energies can be illustrated in a system formed by two shells of the same degeneracy

with a number of particles great enough to fill one of them, and by considering only the quadrupole–quadrupole hamiltonian. If they are degenerate, one will find that $a_0^2 = 0.5$ as in the one-shell situation. On the other hand if their energy difference is big enough a_0^2 will be equal to one because it is a closed-shell system.

We want to thank D.R. Bès and R.P.J. Perazzo for helpful discussions and comments.

References

1) D.R. Bès, G.G. Dussel, R.A. Broglia, R.J. Liotta and B.R. Mottelson, Phys. Lett. **52B** (1974) 253
2) L. Landau, J. Phys. (USSR) **5** (1941) 71
3) P.F. Bortignon, R.A. Broglia and D.R. Bès, Phys. Lett. **76B** (1978) 153
4) G.G. Dussel and D.R. Bès, Nucl. Phys. **A323** (1979) 392
5) A. Bohr and B. Mottelson, Phys. Scripta **22** (1980) 468;
R.A. Broglia, Microscopic structure in the intrinsic state of a deformed nuclei, preprint
6) A. Arima and F. Iachello, Ann. of Phys. **99** (1976) 253; **111** (1978) 20
7) K. Kumar and M. Baranger, Nucl. Phys. **A110** (1968) 529
8) P.C. Martin and J. Schwinger, Phys. Rev. **115** (1959) 1342
9) J. Dukelsky, G.G. Dussel and H.M. Sofía, Phys. Lett. **100B** (1981) 367
10) M. Barard and N. de Takacsy, Phys. Rev. **C20** (1979) 2439
11) T. Otsuka, Rotational states and interacting bosons, preprint